Supporting Information

Architecting an Electron Highway: Cobalt-Doped Tubular Carbon Nitride for Superior Photocatalytic PMS Activation

Jiani Qin[a*], Minna Duan[a], Jianping Zhang[b], Wen Chen[a], Tingjiang Yan[b], Chuanyi Wang[a, d*], Bao Pan[b,c*]

[a] School of Environmental Science and Engineering, Shaanxi University of Science and Technology, Xi'an 710021, P. R. China.

[b] School of Chemistry and Chemical Engineering, Shaanxi University of Science and Technology, Xi'an 710021, P. R. China.

[c] Engineering Research Center of Biofilm Water Purification and Utilization Technology of Ministry of Education, Anhui University of Technology, Ma'anshan 243032, P. R. China.

[d] Department of Environmental and Sustainable Engineering, Faculty of Engineering, Chulalongkorn University, 254 Phayathai Road, Pathumwan, Bangkok, 10330, Thailand.

Email: jianiqin@sust.edu.cn; wangchuanyi@sust.edu.cn; panbao@sust.edu.cn

Characterizations

The powder X-ray diffraction (XRD) patterns of the samples were obtained on a SmartLab diffractometer (Rigaku, Japan). The Fourier transform infrared spectra (FT-IR) of the samples in the range of 4000-400 cm^{-1} were recorded on a Bruker Invenio spectrometer with KBr as background. The X-ray photoelectron spectra (XPS) were measured on a Thermo ESCALAB 250XI spectrometer with an Al Kα line source to analyze the elemental composition and valence state changes. XPS analysis was performed on multiple independently synthesized batches of the representative catalysts to confirm the reproducibility of the surface chemical states. The total organic carbon (TOC) in the solution was measured by a Liqui TOC II analyzer (Germany) to analyze the mineralization degree of the reaction system. The Brunauer-Emmett-Teller (BET) was measured by a Micromeritics ASAP 2460 to determine the specific surface area, pore volume and pore size distribution of the catalyst. The morphology of the samples was collected on a Sigma360 scanning electron microscope (SEM). The electron paramagnetic resonance (EPR) analysis was carried out using a Bruker E500-10/12 spectrometer. The intermediate products during the degradation process were detected by HPLC-MS (Waters ZQ-2000).

Electrochemical measurements were carried out using an electrochemical workstation (Guangzhou Ingsens Sensor Technology Co., Ltd., IGS 4030). An Ag/AgCl electrode was used as the reference electrode, a 10 × 10 mm^2 Pt sheet as the counter electrode, and catalyst-loaded tin oxide fluorine (FTO) as the working electrode. 0.5 M sodium sulfate (Na_2SO_4) solution was used as the electrolyte.

The XAFS (X-ray Absorption Fine Structure) data were analyzed using the Demeter software package, which includes Athena for XANES (X-ray Absorption Near Edge Structure) analysis and Artemis for EXAFS (Extended X-ray Absorption Fine Structure) analysis. An amplitude reduction factor ($S0^2$) of 0.73, derived from EXAFS analysis of Co foil, was then fixed as a parameter in the fitting of the EXAFS data.

Transmission XAS measurements were performed on a laboratory device (easyXAFS300+, easyXAFS LLC), which is based on Rowland circle geometries with spherically bent crystal analyzers (SBCA) and a silicon drift detector. Si(5,3,3) was used for Co K-edge measurement. The powder samples were thoroughly ground and mixed with Boron Nitride using an agate mortar and pestle and pressed into Ø = 10 mm pellets. The pressed pellets were then sandwiched by Kapton tapes.

Figures and Tables

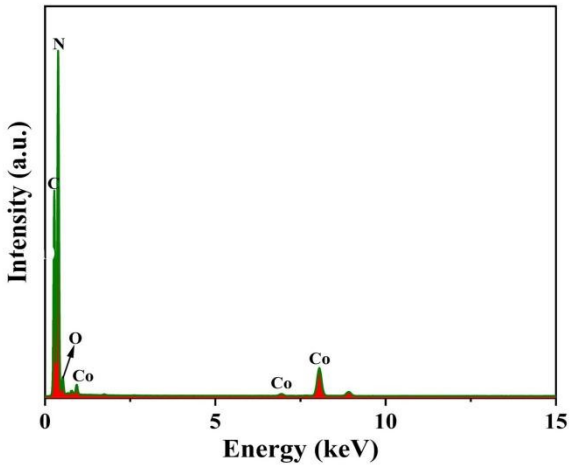

Fig. S1 EDS of 1.1%Co-TCN.

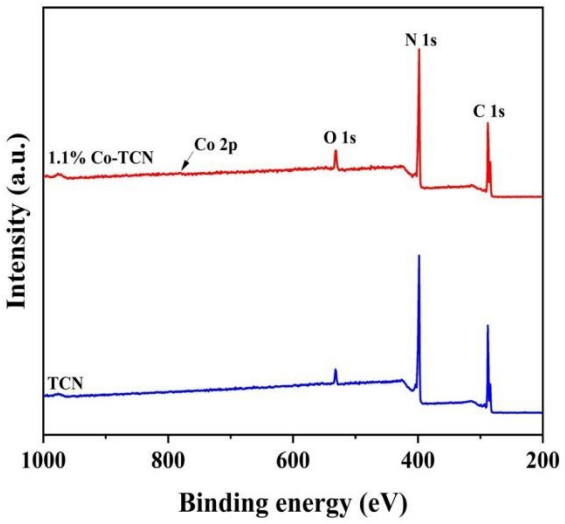

Fig. S2 The XPS full spectra of TCN and 1.1%Co-TCN.

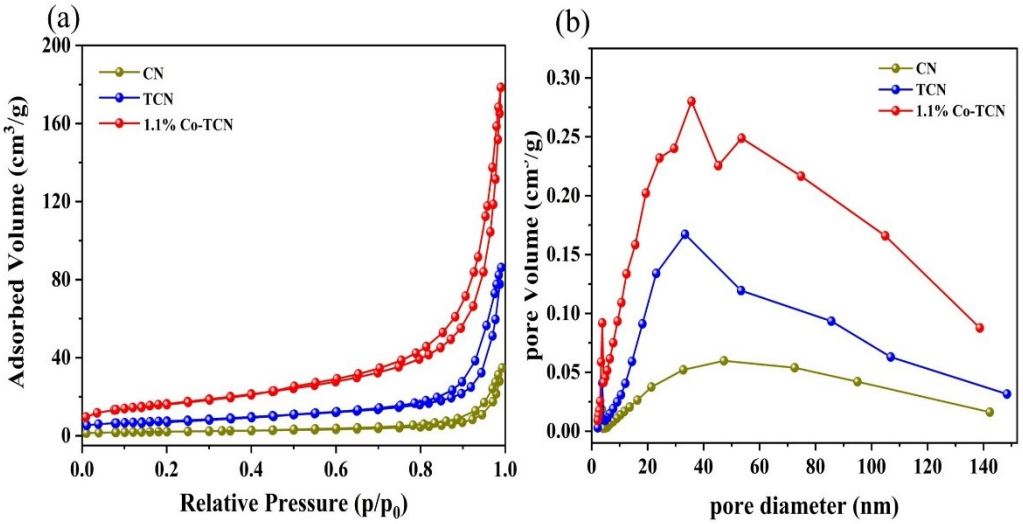

Fig. S3 N_2 adsorption-desorption isotherms (a), corresponding pore size distribution (b) of CN, TCN, and 1.1%Co-TCN.

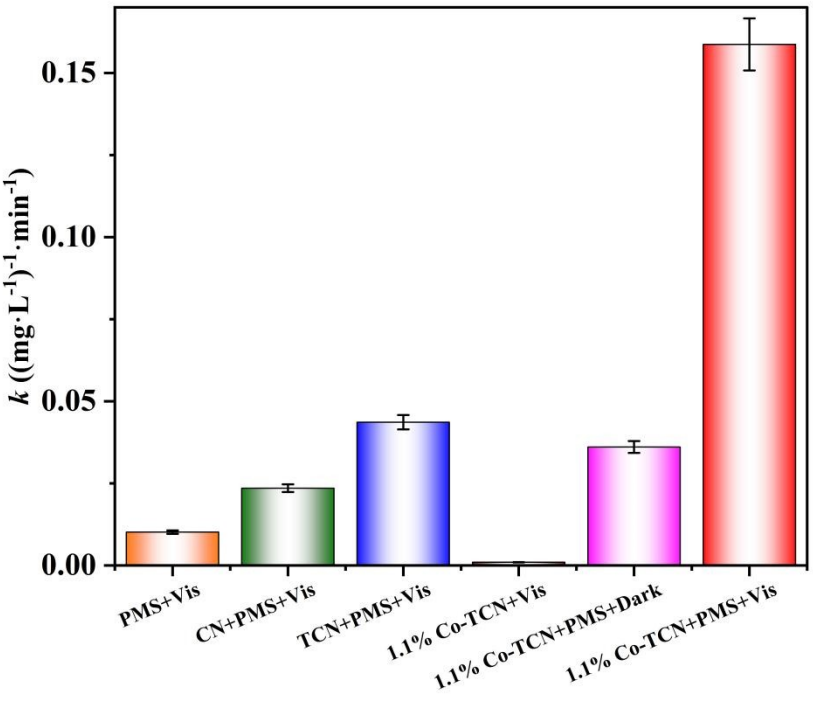

Fig. S4 Reaction rate constant over different reaction systems.

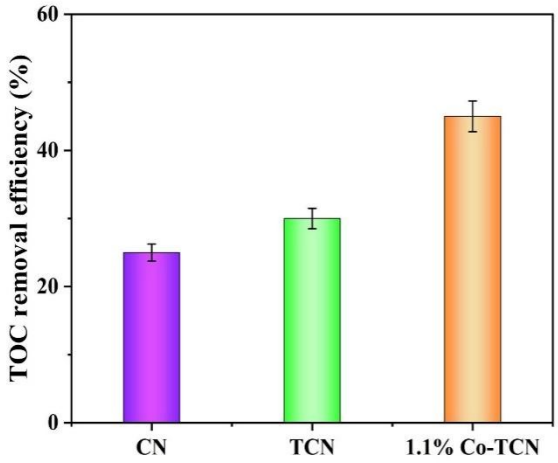

Fig. S5 TOC removal efficiency of CN, TCN and 1.1% Co-TCN.

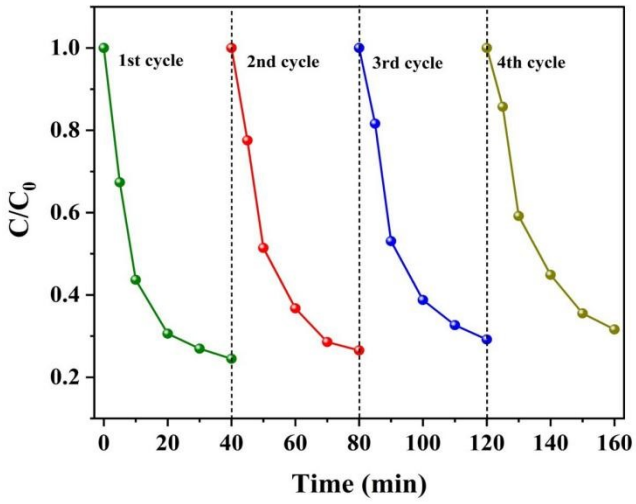

Fig. S6 Cyclic experiment of photocatalytic activation of PMS by 1.1%Co-TCN for the degradation of TC.

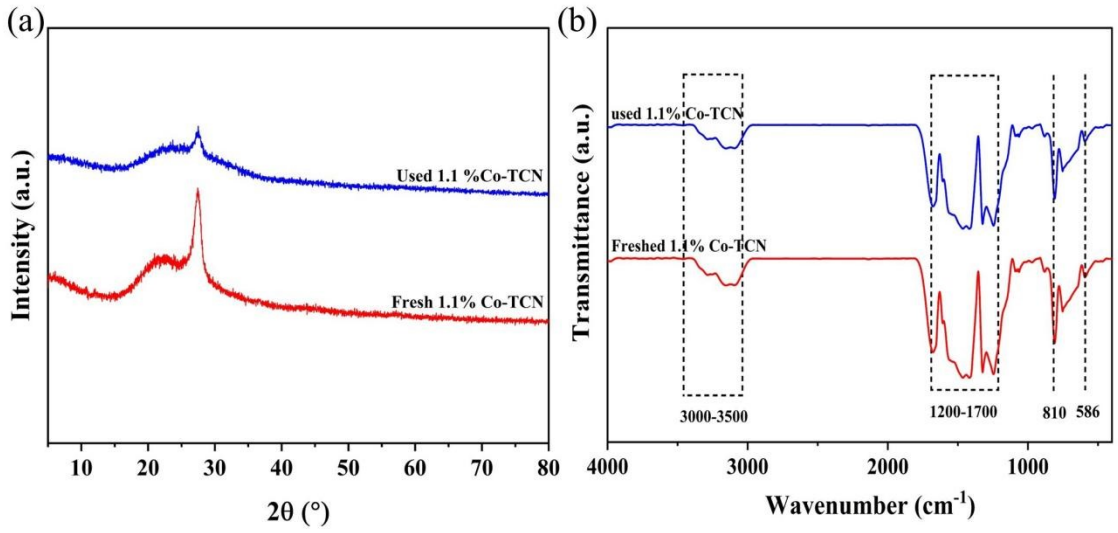

Fig. S7 (a) XRD patterns, (b) FT-IR spectra of fresh and used 1.1%Co-TCN.

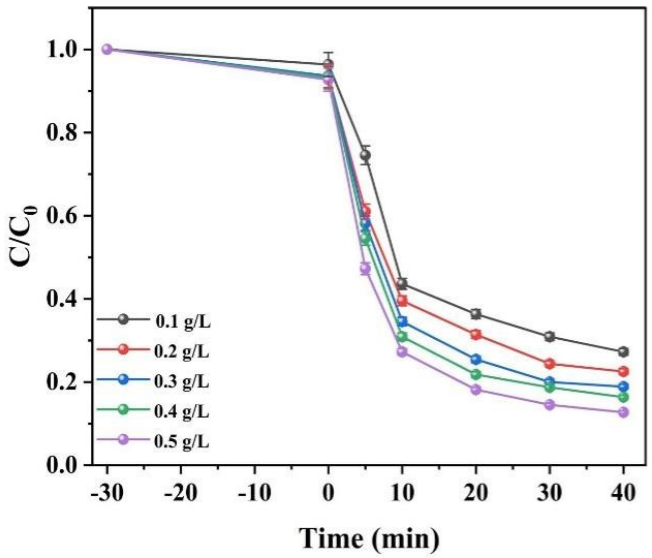

Fig. S8 Effects of 1.1%Co-TCN dosage on TC degradation.

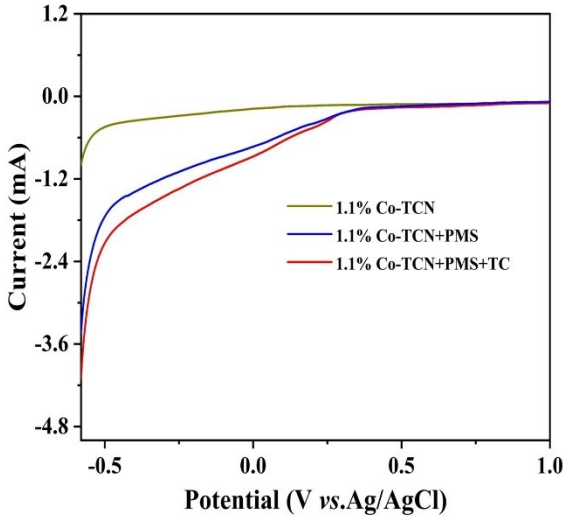

Fig. S9 LSV curves of 1.1%Co-TCN under different conditions.

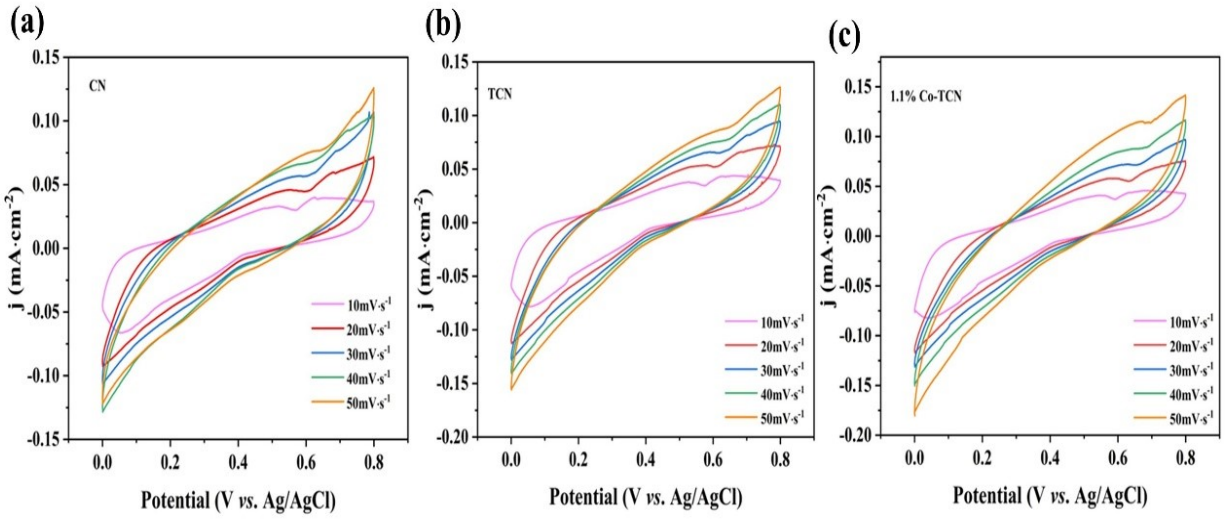

Fig. S10 CV curves of (a) CN (b) TCN and (c) 1.1%Co-TCN at different scan rates.

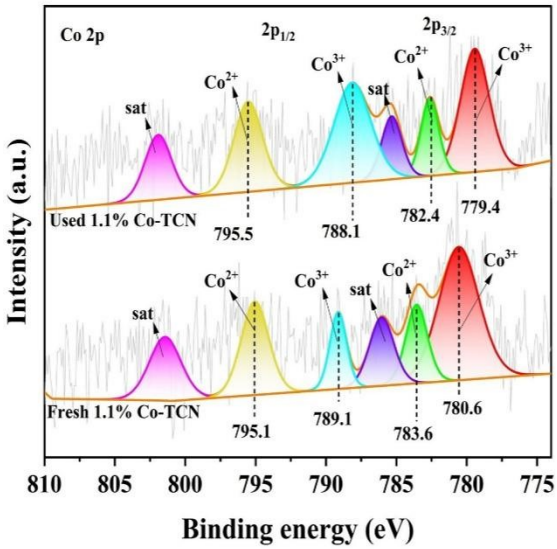

Fig. S11 High-resolution Co 2p XPS spectra of fresh and used 1.1%Co-TCN.

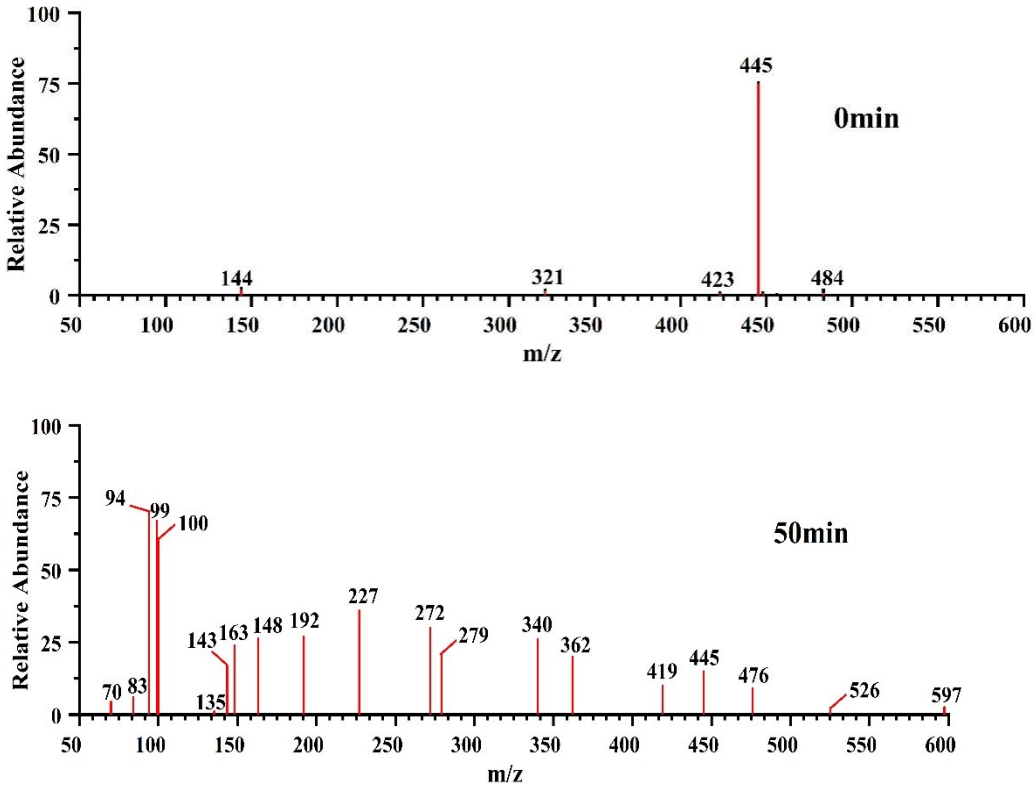

Fig. S12 HPLC-MS spectra of TC degradation intermediates with different times.

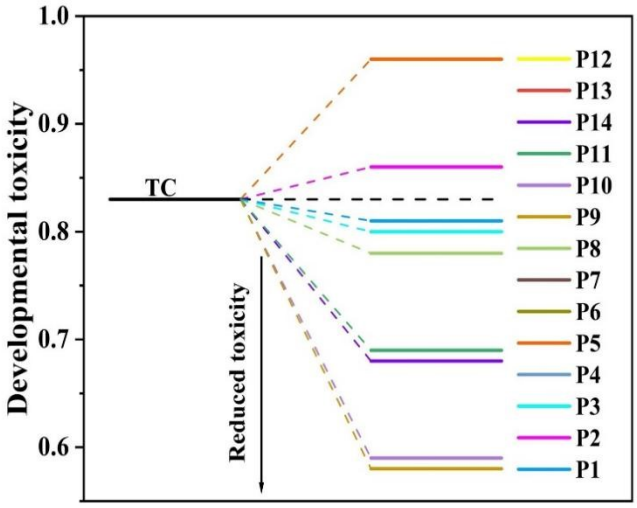

Fig. S13 Developmental toxicity of TC and degradation intermediates in the 1.1%Co-TCN+PMS+Vis system.

Table S1. Fitting parameters of EXAFS for cobalt K-edge

Samples	Path	C.N.[a]	R(Å)[b]	σ^2(10^{-3} Å^2)[c]	R factor[d]
Co	Co-O	4.2±0.5	2.03±0.02	5.0±1.0	0.008

[a]C.N.: coordination numbers; [b]R: bond distance; [c]σ^2: Debye-Waller factors; [d]R factor: goodness of fit.

S_0^2 was set as 0.73 for Co data, which was obtained from the experimental EXAFS fit of Co foil reference by fixing CN as the known crystallographic value and was fixed to all the samples.

Table S2. S_{BET}, pore volume, and average pore size of samples.

Sample	S_{BET} (m^2/g)	Pore volume (m^3/g)	Average pore size (nm)
CN	7.2877	0.56772	26.8866
TCN	26.0317	0.14339	21.5480
1.1%Co-TCN	58.2348	0.29849	18.7853

Table S3. Comparison of the degradation of micro-pollutants by reported TCN-based photocatalysts.

Catalysis	Oxidizing agent	Pollutant	Light source	Irradiation time	Photodegradation efficiency	Ref.
Co-TCN	PMS	20 mg/L TC	300 W Xe lamp	40 min	77.4%	This work
g-C_3N_4/ $MnIn_2S_4$	PMS	20 mg/L TC	300 W Xe lamp	40 min	72.8%	[1]
g-C_3N_4/ Bi_3O_4Cl	PMS	10 mg/L TC	60 W Xe lamp	60 min	76%	[2]
CNT	PMS	20 mg/L TC	60 W Xe lamp	180 min	55%	[3]
g-C_3N_4/ ZnO	---	30 ppm MB	150W Xe lamp	70 min	73.83%	[4]

Table S4. The peak position, FWHM and area ratio of 1.1%Co-TCN.

1.1% Co-TCN		peak positions (eV)	FWHM	area ratios (%)
Co^{3+}	Before the reaction	780.6; 789.1	3.50; 1.65	49
	After the reaction	779.4; 788.1	3.20; 2.66	51
Co^{2+}	Before the reaction	783.6; 795.1	3.42; 3.50	51
	After the reaction	782.4; 795.5	3.50; 3.50	49

References

[1] X.Xiao, Y. Wang, H. Zhang, Z. Chou, H. Ding, X. Lu, Y. Zou, L. Chen and D. Sun, J. Alloys Compd., 2025, 1022, 179835.

[2] H. Che, G. Che, H. Dong, W. Hu, H. Hu, C. Liu, C. Li, Fabrication of Z-scheme Bi_3O_4Cl/g-C_3N_4 2D/2D heterojunctions with enhanced interfacial charge separation and photocatalytic degradation various organic pollutants activity, Appl. Surf. Sci. 455 (2018) 705-716.

[3] Y. Wang, M.Farooq, H. Kosslick, T. Beweries, A. Schulz, S. Tschierlei, Synthesis and comparative study of the photocatalytic performance of hierarchically porous polymeric carbon nitrides, March 201.488(2015) 801-812.

[4] X. Guo, J. Duan, C. Li, Z. Zhang, W. Wang, Highly efficient Z-scheme g-C_3N_4/ZnO photocatalysts constructed by co-melting-recrystallizing mixed precursors for wastewater treatment, J. Mater. Sci. 55 (5) (2020) 2018-2031